

PROCEEDINGS OF SPIE

SPIDigitalLibrary.org/conference-proceedings-of-spie

Development of remote sensing satellite attitude visualization simulator: mechanical design

Rianto, Puji, Herawan, Agus, Kurniawan, Rendy, Utama, Satriya

Puji Rianto, Agus Herawan, Rendy Kurniawan, Satriya Utama, "Development of remote sensing satellite attitude visualization simulator: mechanical design," Proc. SPIE 11372, Sixth International Symposium on LAPAN-IPB Satellite, 113721Y (24 December 2019); doi: 10.1117/12.2542655

SPIE.

Event: Sixth International Symposium on LAPAN-IPB Satellite, 2019, Bogor, Indonesia

Development of Remote Sensing Satellite Attitude Visualization Simulator: Mechanical Design

Puji Rianto^{*a}, Agus Herawan^a, Rendy Kurniawan^a, Satriya Utama^a

^a Satellite Technology Center, Indonesian National Institute of Aeronautics and Space (LAPAN), Bogor, Indonesia 16310

ABSTRACT

LAPAN already has three satellites in orbit. All the LAPAN Satellites are remote sensing satellite that will send satellite attitude data in real time mode and offline mode. The satellite attitude data is very important in a remote sensing satellite mission. For example, in the digital imager mission, operator use attitude data to take the image of targeted area with high accuracy. To make it easier for operators to understand satellite attitude, they need a satellite simulator or satellite mock up that can show satellite attitudes in realtime or offline mode, especially in special missions. In addition, the dissemination division can also use the simulator to educate people about satellites. This paper discusses the working principle of the simulator and the structural design of the simulator. After the analysis, it is obtained that simulator uses the gimbal mechanism. The materials for the structure is 7075-T6 aluminum alloy. Meanwhile, the drive are three 17HS4401 stepper motor in each axis. The 17hs4401 stepper motor is strong enough to rotate all axes and the 7075-T6 aluminum alloy is strong enough and rigid to be used as a simulator structure.

Keywords: LAPAN Satellite, Remote Sensing, Satellite Attitude Data, Simulator, Gimbal Mechanism

1. INTRODUCTION

LAPAN already has three satellites in orbit, LAPAN-A1, LAPAN-A2 and LAPAN-A3. The three satellites has several mission with one common mission, they has cammera for remote sensing. LAPAN-A1 has two cammeras for surveillance mission¹, already launched in 2007 with many achievement such as taking a picture of Singapore Changi Airport in 2007. LAPAN-A2, launched in 2015², equiped with high resolution matrix camera that used for several mission such as monitoring toll road cunstruction in Java³. Meanwhile, LAPAN-A3 which launched 1 year after LAPAN-A2, bring multispectral imager, mainly for vegetation monitoring in Indonesia⁴. Compared to the predecessor satellite, LAPAN-A3 is the most widely usage, with some application such as land cover classification over Lake Toba area of North Sumatra⁵

To achieve the mission, LAPAN satellites are operated from main ground station in Bogor with suport from other ground station such as Agam, Parepare, Biak and Spizbergen. A remote sensing satellite operator must understand the attitude of the satellite. That is because attitude data plays a key role for spacecraft⁶ and determining the target area, an operator must know the attitude of the satellite so that the satellite camera sweep area in accordance with area of interest. In addition to the accuracy in taking pictures, the speed in making or changing mission must be done to avoid taking pictures that only contain clouds^{7,8}. From these problems, it is necessary to have a tool that can facilitate the operator. Tools that can create simulation and 3D visualization are much helpful to ensure the feasibility and reliability of the mission planning and to improve the efficiency of the satellite utilization⁹. The tool is in the form of a satellite simulator that can display satellite attitudes both in realtime and off line with the input in the form of satellite attitude data and ground track satellite based on Two Line Element (TLE). In addition to displaying satellite attitudes, the simulator must be able to display the approximate area of the satellite camera sweep. Besides being useful for operators, simulators are very useful in the field of dissemination. The Dissemination Division can utilize the simulator as an educational media about satellites.

Some simulator are already done in LAPAN, but none of them are using a satellite mock up to visualize the attitude, most of them are only software simulator. A simulator for LAPAN-A1 (LAPAN-Tubsat) already built with aim to help satellite operator to understand video analog mission on the satellite¹⁰. Started in 2012 LAPAN worked with ITB to built a satellite

simulator, especially for the attitude module¹¹. Another work already use satellite telemetry as input for satellite attitude¹², although the visualization only use a 3D graph.

2. MODELING AND LOAD CASE ANALYSIS

The most common way to represent the attitude of a rigid body is a set of three Euler angles. These are popular because they are easy to understand and easy to use. Some sets of Euler angles are so widely used that they have names that have become part of the common parlance, such as the roll, pitch, and yaw. Therefore, to show yaw, pitch and roll from a satellite, the simulator was developed using a three axis gimbal mechanism so that the simulator has three degrees of freedom.

The simulator is modeled using CAD Software based on research that has been done¹³. Figure 1 is a simulator design created. The design consists of the base structure (b) which is the place where the gimbal structure, the controller (a) and the display screen (k) are placed. Gimbal structure consists of outer gimbal (d) which represents satellite yaw motion, inner gimbal (h) represents pitch motion, while rotary table (i) represents roll motion on satellite. In the outer gimbal and inner gimbal there are three counterweight (f) (l) which is useful for positioning the mass center as close as possible to the rotation axis of each gimbal mechanism. The simulator uses three stepper motors (c) (e) (j) to move the mechanism. Especially on motor yaw (c) and pitch (e) there is a 3: 1 reduction pulley to increase torque. A satellite mockup (g) is mounted on the rotary tabl to display the satellite's attitude.

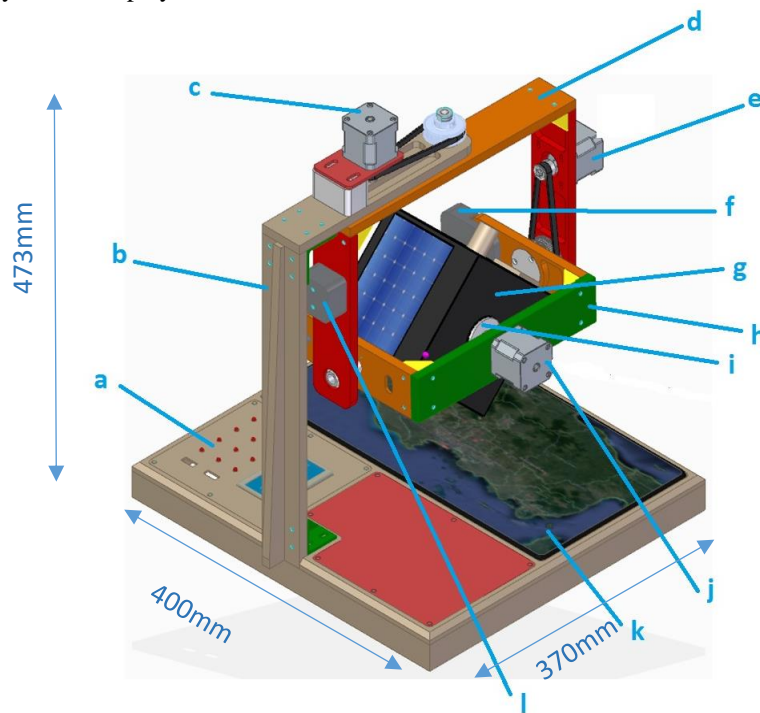


Figure 1. 3D model of simulator

The working principle of the simulator in general, operators enter satellite attitude data whether real time or off line through the control panel. In addition to satellite attitude data, operators must enter TLE data according to the satellite attitude data date. The controller will process the satellite attitude data into two types of commands: first, the command for three motor gimbal mechanisms (yaw, pitch, roll) in the form of steps and second, the command for the display screen to shift the map display on the screen.

The center of gravity of the gimbal mechanism must be as close as possible to the axis of rotation. Central of gravity can be shifted by adding a counterweight. In determining the position and size of the counterweight, the calculation must be repeated so that the position of the center of gravity is very close to the axis of rotation. COG calculations are performed using one of the features in CAD Software.

Simulator structure material must be strong and lightweight so that the size of the driving motor used can be as small as possible. The 7075-T6 aluminum alloy is a material that is widely used in aircraft structures due to their high strength-to-weight ratio. The 7075-T6 aluminum alloy has a 572MPa Ultimate Tensile Strength and 503MPa Yield Tensile Strength. Therefore the structure of the simulator is made of 7075-T6 aluminum alloy. That way the weight of the simulator will be light, especially on the gimbal mechanism. The advantage of the lighter gimbal mechanism is that the moment of inertia gets smaller as well as the load of the driving motor gets smaller, so that the size of the stepper motor that will be used can be as small as possible. That is because the stepper motor has a limited holding torque.

The analysis of structural strength uses CAE Software. The analysis is divided into three sub-assemblies, namely base structure, yaw structure and pitch structure. The load case for each sub-assy can be seen in Table 1. While Table 2 is the mechanical property data of Aluminum 7075-T6. In summary, the workflow of the simulator design process can be seen in Figure 2.

Table 1. Analysis structure load case

Load case	Load				Explanation
	Base assembly	Yaw assembly	Pitch assembly	Roll assembly	
Base Structure	v	v	v	v	-
Yaw Structure		v	v	v	-
Pitch Structure 1			v	v	when the roll axis is in line with the yaw axis
Pitch Structure 2			v	v	when the roll axis is perpendicular to the yaw axis

Table 2. Mechanical properties of Aluminium 7075-T6¹⁴

Item	Value	Unit
Density	2810	kg/m ³
Ultimate Tensile Strength	572	MPa
Tensile Yield Strength	503	MPa
Poisson's Ratio	0.33	-
Modulus of Elasticity	71.7	Gpa

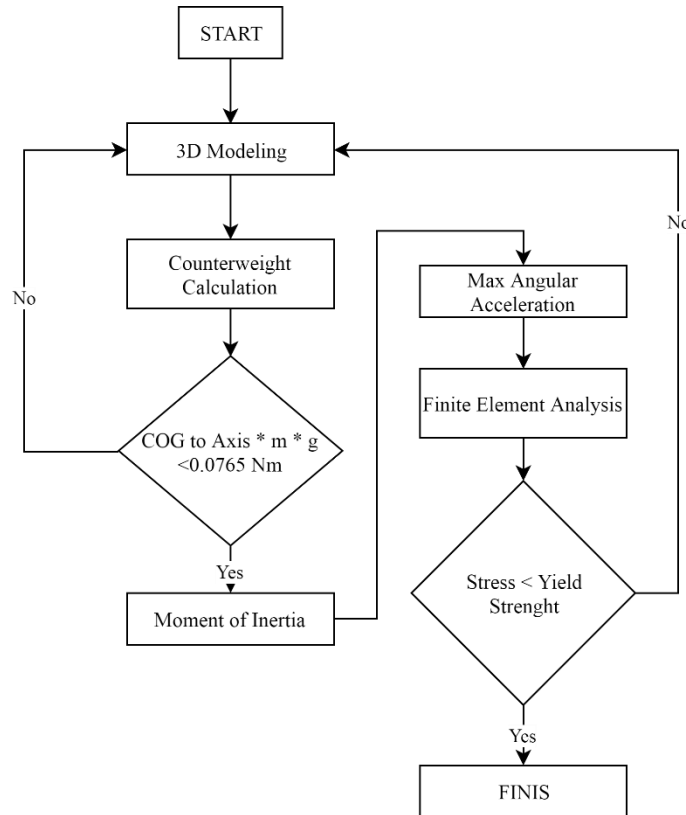


Figure 2. The workflow of the simulator design process

3. DATA AND ANALYSIS

3.1 COG, Moment of Inertia, and Angular Acceleration

Table 3 shows the comparison between the design before and after adding a counterweight. From the data in Table 3, we can see the difference between after and before adding a counterweight. One of the main objectives of adding a counterweight is to maintain the moment arising from unbalanced loads of less than half the holding torque of the stepper motor. It is intended that the safety factor of a stepper motor is at least 2. The simulator uses a 17HS4401 stepper motor with a holding torque of 0.4Nm so that the torque received by the motor due to unbalanced mass must not exceed 0.2Nm. To increase the accuracy of the simulator, the motor uses a quarter of microstepping. So that initially each step is worth 1.8 degrees and becomes 0.45 degrees after using a quarter of microstepping. However, due to the use of microstepping, holding torque becomes 38.27% of holding torque when using fullstep. So that the maximum allowable torque received by the motor is 0.077Nm so that the mistep can be minimized.

By using the formula¹⁵ $\tau = \frac{1}{3} F \times d$, on yaw and pitch, where τ is torque, $\frac{1}{3}$ is the value of the pulley ratio on the yaw and pitch axis, F is the load due to gravitational force and d is the distance between COG and rotary axis. From these calculations the torque received by the motor yaw is 0.00375Nm and the motor pitch is 0.00677Nm. Whereas the moment on the roll axis uses $\tau = F \times d$, because there is no reduction pulley. With this equation, the moment received by the motor roll is 0.0155Nm. With these three values, it can be concluded that the motor 17HS4401 is able to maintain the position of the simulator assuming there is no outside interference.

Table 3. Before and after the counterweight was added

Item	Load (N)		COG to axis (mm)		Moment of Inertia (kg.m ²)	
	Before	After	Before	After	Before	After
Yaw Structure	29.03	32.11	17.51	0.35	0.04388	0.05218
Pitch Structure	12.92	18.81	114.82	1.08	0.03129	0.01102
Roll Structure	3.78	-	4.11	-	0.00166	-

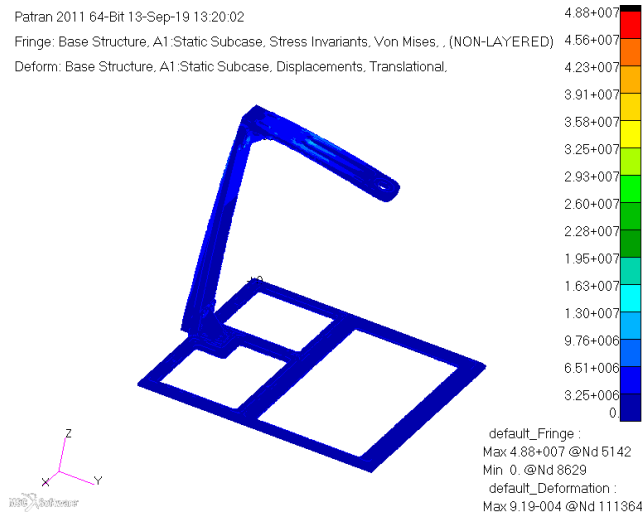
After completing the ability of the motor 17HS4401 to maintain its position, the thing to note is the ability of the motor to accelerate and decelerate. When a stepper motor is forced to accelerate and decelerate beyond the limits of the motor's ability, then a misstep will very likely occur. On the other hand, when acceleration and decelerate are too slow to avoid missteps, the simulator response will be slow. For this reason, it is necessary to calculate the maximum acceleration and deceleration which can be done by the motor.

From Table 3, it can be seen that the addition of a counterweight that aims to bring the COG closer to the rotary axis causes the moment of inertia on the rotary axis to increase. Because the moment of inertia is directly proportional to the mass of an object. Based on the formula $\tau = \frac{1}{3}I \times \alpha$, where τ is torque, $1/3$ is the pulley ratio for yaw and pitch, I is the moment of inertia while α is the angular acceleration. The difference in maximum acceleration before and after the counterweight is added can be seen in Table 4. The angular acceleration obtained can be used as a limitation in creating a motor speed profile to avoid missteps.

Table 4. Maximum acceleration

Item	Maximum acceleration (rad/s ²)	
	Before	After
Yaw	5.26	4.43
Pitch	32.31	20.96
Roll	46.39	-

3.2 Structural Strenght Analysis



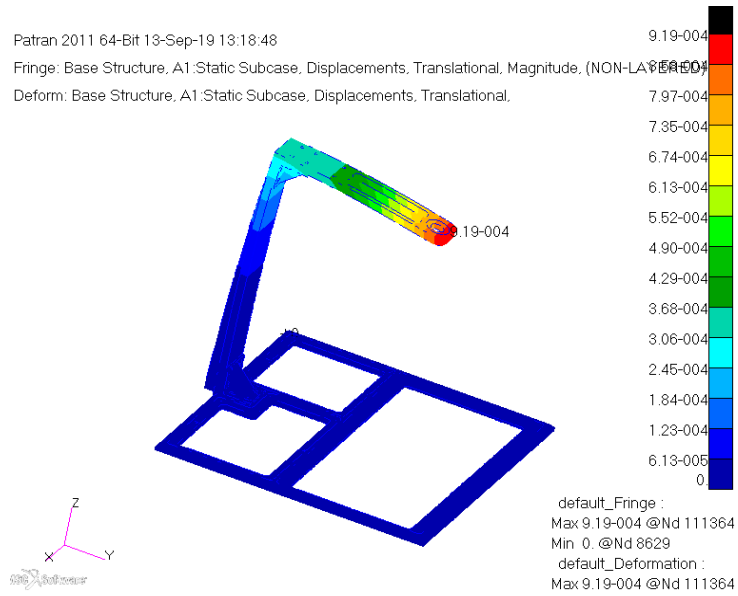
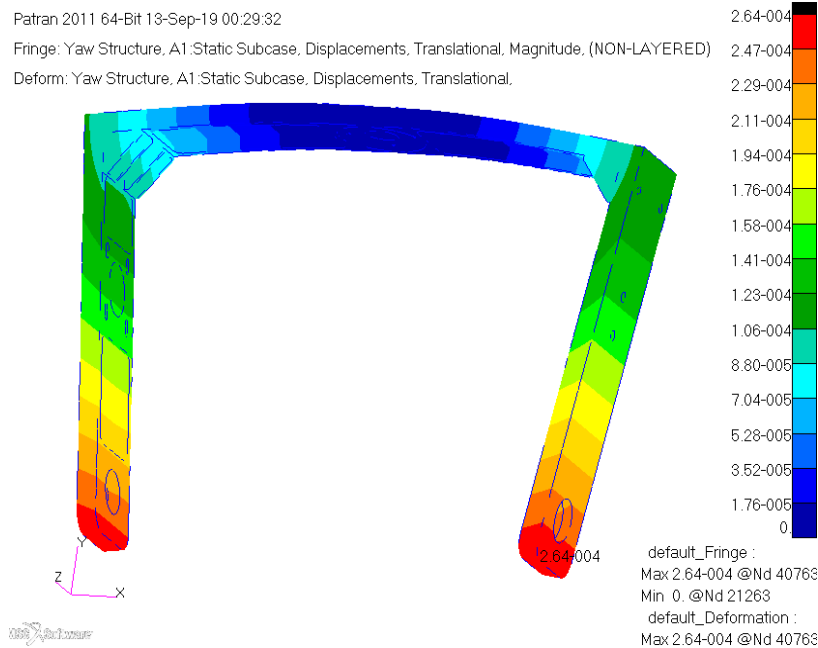


Figure 3. Result of base structure load case

Figure 3 is the result of finite element base structure analysis with the case of loading "base structure". The strength and stiffness of the base structure is very important because the base structure on which the gimbal mechanism is hung. When the base structure is not strong enough, the simulator cannot be used. After conducting a static load analysis, the base structure has a maximum stress of 48.8 MPa and a maximum displacement of 0.919 mm. The strength of the base structure is very strong because the safety factor is more than 10 times but for the stiffness of the base structure it is less rigid because it has a displacement of almost 1mm. Even so with a displacement of 0.919mm the base structure is still feasible to use.



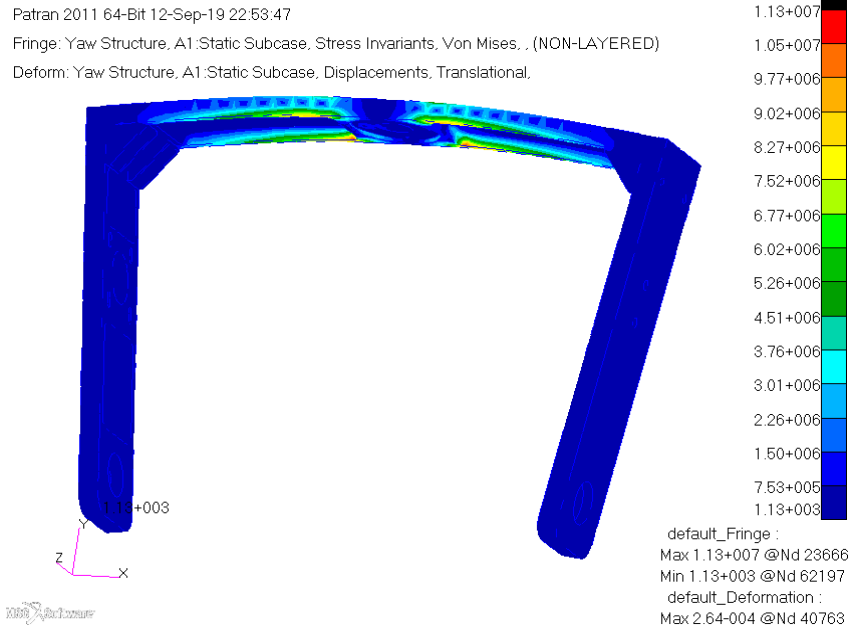
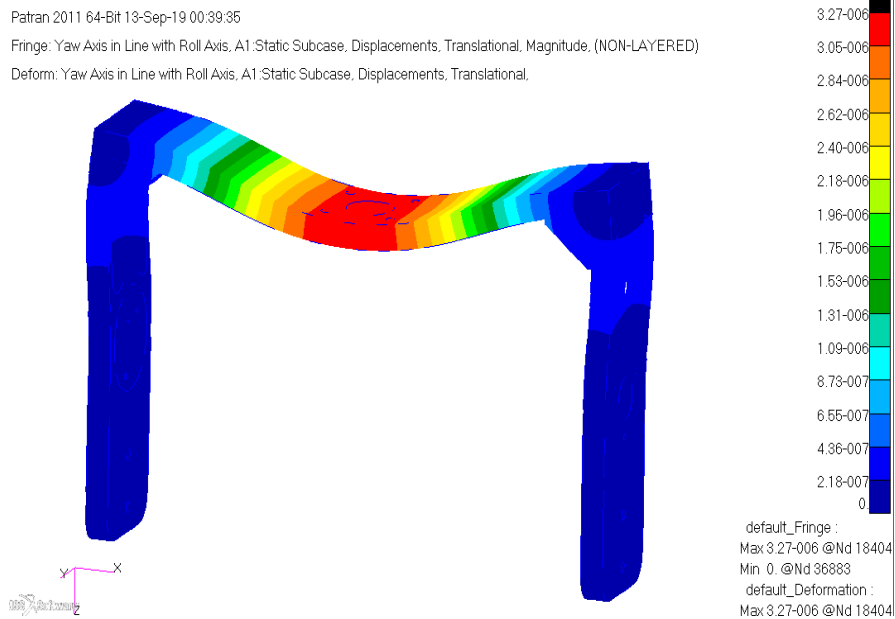


Figure 4. Result of yaw structure load case

Figure 4 is the result of the analysis of the yaw structure where the maximum stress is 11.3 MPa and the maximum displacement is 0.264 mm. With a yield strength of Al7075-T6 of 503Mpa, the structure is very safe and rigid. The maximum stress occurs around the yaw's axis. This happens because at that location there is a hole that is used as a cable line besides that location there is also a depletion of the material to reduce mass. Mass reduction is done to reduce the moment of structural inertia. So that the motor can accelerate and decelerate faster, in other words the simulator can provide a faster response when input data is entered.



Patran 2011 64-Bit 13-Sep-19 00:41:09

Fringe: Yaw Axis in Line with Roll Axis, A1:Static Subcase, Stress Invariants, Von Mises, (NON-LAYERED)

Deform: Yaw Axis in Line with Roll Axis, A1:Static Subcase, Displacements, Translational.

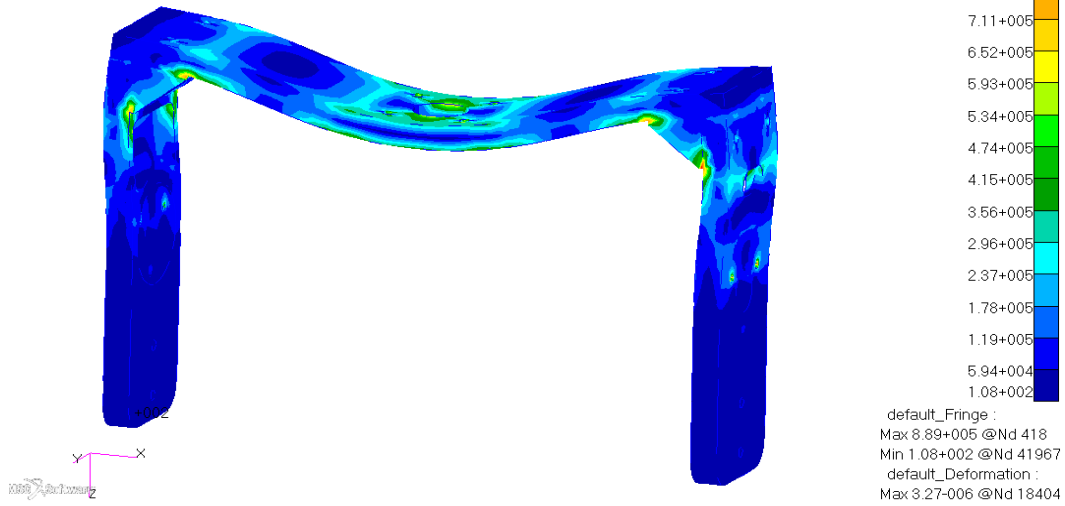


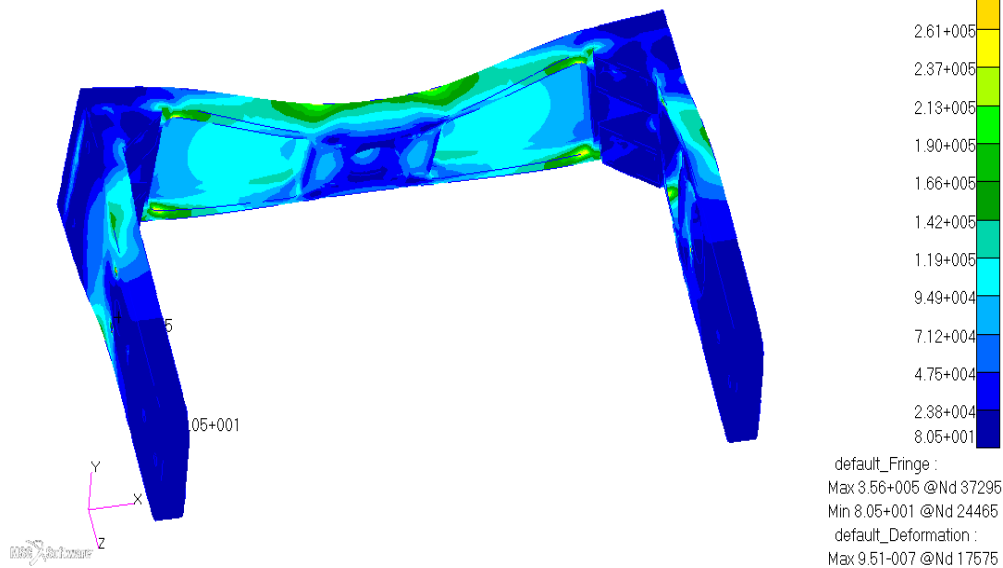
Figure 5. Result of pitch structure 1 load case

Figure 5 displays the pitch structure after simulating the pitch structure1 load case. The maximum stress that occurs is 0.889 MPa and the maximum displacement that occurs is 3.27e-3mm. When compared with the strength yield of 503 MPa and the static load analysis of the design can be said to be very safe. Displacement that occurs in the structure is also very small so that it can be concluded the design of the pitch structure is made very rigid if analyzed based on pitch structure1 load case. if the analyst results are compared with load case 1, load case 2 has better results as shown in figure 6. This shows that the structure is more rigid when the pitch angle is 0 degrees compared to when the pitch angle is 90 degrees.

Patran 2011 64-Bit 13-Sep-19 00:46:05

Fringe: Yaw Axis Perpendicular to Roll Axis, A1:Static Subcase, Stress Invariants, Von Mises, (NON-LAYERED)

Deform: Yaw Axis Perpendicular to Roll Axis, A1:Static Subcase, Displacements, Translational.



Patran 2011 64-Bit 13-Sep-19 00:43:12

Fringe: Yaw Axis Perpendicular to Roll Axis, A1:Static Subcase, Displacements, Translational, Magnitude, (NON-LAYERED)

Deform: Yaw Axis Perpendicular to Roll Axis, A1:Static Subcase, Displacements, Translational.

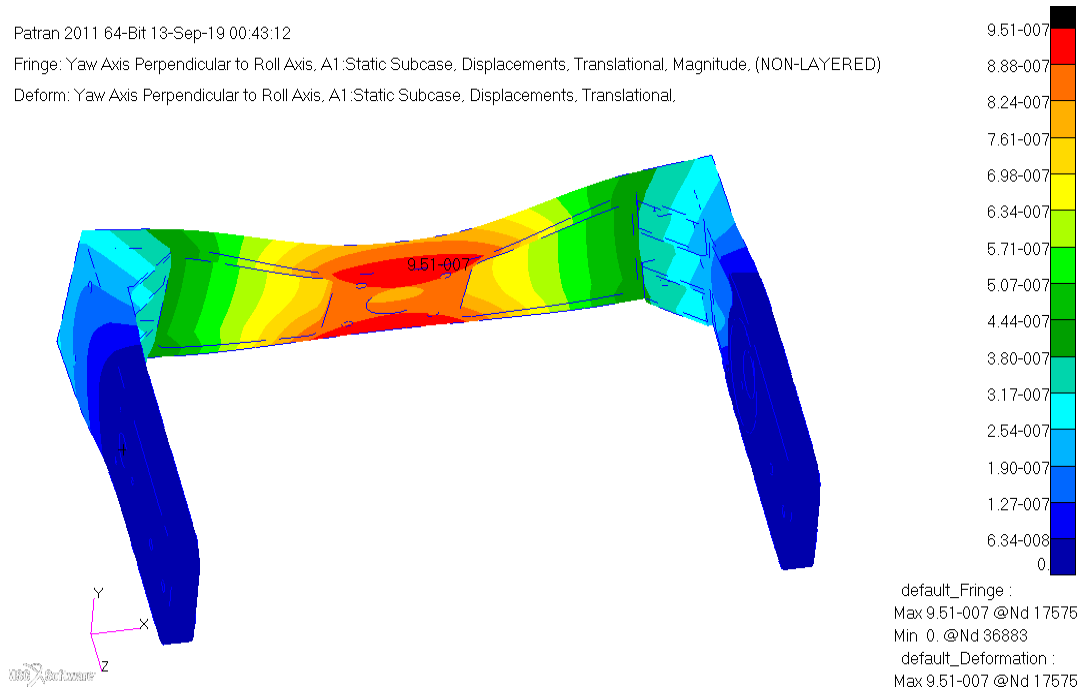


Figure 6. Result of pitch structure 2 load case

4. CONCLUSION

Based on the explanation above, it can be concluded that 7075-T6 Aluminum alloy as a material for the simulator structure is very good although there is a deflection of 0.919 mm. The design can be changed in the future if the deflection value causes problems. The selection of stepper motor 17HS4401 is strong enough to move the gimbal mechanism. With the largest acceleration found on the roll axis that is 46.39 rad / s.

REFERENCES

- [1] Triharjanto, R., Hasbi, W., Widipaminto, A., Mukhayadi, M., and Renner, U., "Lapan-Tubsat : micro-satellite platform for surveillance & remote sensing", Proceedings of The 4S Symposium: Small Satellites, Systems and Services (ESA SP-571), (2004).
- [2] Hardhienata, S., Triharjanto, R., H., and Mukhayadi M., "LAPAN-A2 : Indonesian Near-Equatorial Surveillance Satellite" 18th Asia-Pacific Reg. Sp. Agency Forum (APRSF), (2011).
- [3] Wahyudiono, A., and Madina, R., "Utilization of Digital Camera Payload on LAPAN A2 Satellite for Monitoring of Toll Road Construction in Java Island", Seminar Nasional Iptek Penerbangan dan Antariksa XXI, 242-9 (2017).
- [4] Hasbi, W., and Suhermanto, "Development of LAPAN-A3/IPB Satellite an Experimental Remote Sensing Microsatellite", 34th Asian Conf. Remote Sens, (2013)
- [5] Nugroho1, J., T., Zylshal, and Kushardono, D., "Lapan-A3 satellite data analysis for land cover classification (case study: Toba Lake area, North Sumatra)", International Journal of Remote Sensing and Earth Sciences, 15 (1), 71 - 80 (2018).
- [6] Mo, F.,Ye, F., Xie, J., Zhu, H., Liu, R., Jin, J., "A Novel Spacecraft Attitude Recovery Method Based on Platform Vibration", 2019 9th International Conference on Recent Advances in Space Technologies (RAST), 117-122 (2019).
- [7] Gasch, John & Campana, Kenneth, "Cloud cover avoidance in space-based remote sensing acquisition", Proceedings of SPIE - The International Society for Optical Engineering, 336-347,(2000)

- [8] Sakagami, R., Takeishi, N., Yairi T., Hori, K., “Visualization Methods for Spacecraft Telemetry Data Using Change-Point Detection and Clustering”, *Trans. JSASS Aerospace Tech. Japan*, 17 (2), 244-252 (2019).
- [9] Deng, B., Tang, R., Li, J., Yin, E., “Simulation and 3D Visualization of Mission Scheduling for Imaging Satellites”, *Journal of Physics: Conference Series*, 1288, 012038 (2019).
- [10] Hutasuhut, H., M., Utama, S., Mujaddid, S., Poetro, R., E., and Sasongko, R., A., “Pengembangan Simulator Stasiun Bumi LAPAN-TUBSAT”, *Satelit untuk Mitigasi Bencana, Pemantauan Maritim, dan Ketahanan Pangan*, 131–43 (2011).
- [11] Robertus, B., Triharjanto, H., Utama, S., and Poetro, R., E., “Progress on the Development of Micro-Satellite Simulator” *Faculty of Mechanical and Aerospace Engineering , Bandung Institut of Technology*, (2013)
- [12] Utama, S., and Hakim, P., R., “Sun Sensor dan Magnetometer Sebagai Sensor Penentu Sikap Satelit Inklinasi Rendah”, *LAPAN-A2 J. Teknol. Dirgant.* (2018).
- [13] Yue, X., Vilathgamuwa, M., Tseng, K., J., and Nagarajan, N., "Modeling and robust adaptive control of a 3-axis motion simulator", *Conference Record of the 2001 IEEE Industry Applications Conference*, 1, 553-560 (2001).
- [14] “Aluminum 7075-T6; 7075-T651”, *MatWeb*,
<http://asm.matweb.com/search/SpecificMaterial.asp?bassnum=MA7075T6> (23 May 2019).
- [15] Palm III, W., J., “System Dynamics Second Edition”, *Mc Graw Hill, Kingstone*, Chapter 3 (2014).